

Characterization of linear and nonlinear carrier generation in silicon nano-waveguides at 1550 nm

Andres Gil-Molina^{1,2}, Ivan Aldaya^{1,3}, Julián L. Pita², Lucas H. Gabrielli², Hugo L. Fragnito^{1,4}, and Paulo Dainese^{1,*}

¹Gleb Wataghin Physics Institute, ²School of Electrical and Computer Engineering,
University of Campinas, Campinas-SP, 13083-970, Brazil

³Campus São João da Boa Vista, State University of São Paulo (UNESP), 13876-750, SP, Brazil

⁴MackGraphe - Graphene and Nanomaterials Research Center, Mackenzie Presbyterian University, São Paulo-SP, 01302-907, Brazil

*dainese@ifi.unicamp.br

Abstract: We characterize the generation of free-carriers in a silicon strip nano-waveguide at 1550 nm performing pump-and-probe measurements. Compared with bulk silicon, we identified a higher effective two-photon absorption coefficient and a significant carrier-generation via single-photon absorption.

OCIS codes: 130.3130, 130.5990, 250.4390, 130.0130.

Free-carrier absorption (FCA) and free-carrier dispersion (FCD) play an important role in the development of silicon-photonics devices. Although these free-carrier effects are often considered detrimental, for example reducing the efficiency of nonlinear amplification [1], they can also be used to control light within the guiding structure [2]. In strip nano-waveguides, the tight optical confinement leads to enhancement in nonlinear effects [3,4], including two-photon absorption (TPA), which then results in higher generation rate of free carriers. In addition, intra-bandgap states at either the core-clad interface or even in the silicon core allow for free-carrier generation through single-photon absorption (SPA) [5]. In this paper, we present a detailed characterization of free-carrier generation rate on a strip silicon nano-waveguide fabricated in a CMOS foundry. Our experiment, on the one hand, confirms the prediction of an effective TPA coefficient higher than bulk and, on the second hand, accurately characterizes the linear SPA coefficient.

The waveguide under test was fabricated at imec/Europractice and had a cross-section of 450 nm × 220 nm, a 2.4 mm of length, silica cladding and grating couplers at both ends. Two additional samples of different lengths (5.9 and 30 mm) were used to measure coupling (3.7 dB) and propagation (1.4 dB/cm) losses by linear regression at low input power. We implement a pump and probe experimental setup described in [6], with a pulsed pump of 80 ps full-width at half maximum (FWHM) pulse duration and 500 kHz repetition rate at 1547 nm, and a continuous wave (CW) low-power ($\sim 50 \mu\text{W}$) probe at 1549 nm. The input and output pump pulses, and the probe were captured by a wide-bandwidth oscilloscope.

Figure 1a shows the time-resolved probe normalized transmittance, $T(t)$, for different input pump power levels, 100, 360 and 670 mW. The initial fast drop in the transmittance is attributed to non-degenerate TPA [4], whereas the

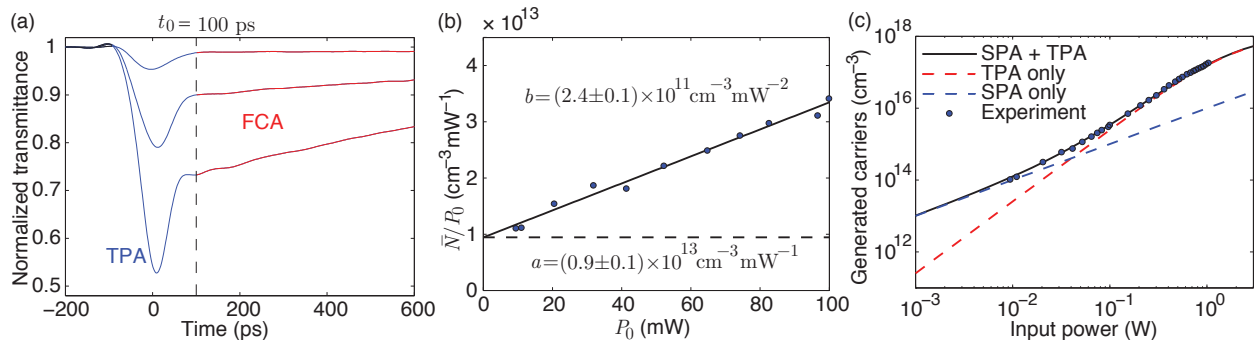


Fig. 1. (a) Normalized probe transmittances for 100, 360 and 670 mW peak pump power; (b) carrier density to power ratio; and (c) generated carriers as a function of input pump power.

following slower regime is dominated by FCA. In order to estimate the amount of generated carriers, we measure the transmittance at $t_0 = 100$ ps, when carrier generation has ceased and before significant recombination has taken place (considering that the measured initial carrier lifetime $\tau_c \approx 800$ ps [6]). Thus, the generated carrier density, averaged along the waveguide length L , was extracted as $\bar{N} = -\ln(T)/(S\alpha_r\eta L)$ [6], where $\alpha_r = 1.45 \times 10^{-17}$ cm 2 is the FCA cross-section at ~ 1550 nm [7], $\eta = 0.77$ is a factor accounting for the mode overlap with the silicon core, and $S = 1.2$ is the so-called slow-light factor that takes into account the enhancement of FCA due to the lower waveguide group velocity compared to that in bulk silicon [4, 8].

In Fig. 1b, we show the generated free-carrier densities for peak pump power levels P_0 ranging from 10 to 100 mW. The data is presented in the form of \bar{N}/P_0 vs. P_0 to explicitly separate linear (through SPA) and nonlinear (through TPA) generation mechanisms. For this power range, \bar{N}/P_0 can be accurately fitted by a linear function of P_0 with non-zero intercept, i.e. $\bar{N}/P_0 = a + b \cdot P_0$. Neglecting pump depletion due to FCA, we can relate the TPA and SPA coefficients, β_{TPA} and α_{SPA} , with the slope b and intercept a obtained from the linear regression (analytical expressions in undepleted regime will be presented somewhere else). The results are $\beta_{TPA} = (1.5 \pm 0.1)$ cm/GW and $\alpha_{SPA} = (1.9 \pm 0.1)$ m $^{-1}$. These parameters were used to numerically calculate the free-carrier density for a wider range of pump power levels (in which FCA induced pump depletion cannot be neglected), and the results compared with our experimental data. The results in Fig. 1c demonstrate that the carrier densities obtained from the numerical model are in good agreement with our measurements up to 1 W. We have also calculated the independent contribution in carrier generation from each mechanism, showing that SPA dominates up to ~ 10 mW, whereas for power levels higher than ~ 300 mW carrier generation is mainly due to TPA. At intermediate power levels, both mechanisms have significant contributions and must be taken into account.

In conclusion, by using time-resolved pump-and-probe measurements, we have characterized the contribution of both TPA and SPA in the generation of free-carriers in a silicon strip nano-waveguide at 1550 nm. Although typical bulk values for β_{TPA} are in the range of (0.4 – 1.2) cm/GW [9], the tight confinement in our nano-waveguide leads to significant enhancement in the effective β_{TPA} [3]. The high effective TPA in combination with non-negligible SPA results in higher generated carrier densities which may be useful in novel applications of light control based on free-carrier effects.

Acknowledgements: FAPESP (2008/57857, 2013/20180-3, and 2015/04113-0), CNPq (574017/2008-9), and CAPES.

References

1. M. A. Foster, A. C. Turner, J. E. Sharping, B. S. Schmidt, M. Lipson, and A. L. Gaeta, “Broad-band optical parametric gain on a silicon photonic chip,” *Nature* **441**, 960–963 (2006).
2. V. R. Almeida, C. A. Barrios, R. R. Panepucci, and M. Lipson, “All-optical control of light on a silicon chip,” *Nature* **431**, 1081–1084 (2004).
3. V. S. Afshar, T. Monro, and C. M. de Sterke, “Understanding the contribution of mode area and slow light to the effective Kerr nonlinearity of waveguides,” *Optics Express* **21**, 18,558–18,571 (2013).
4. Y. Zhang, C. Husko, S. Lefrancois, I. H. Rey, T. F. Krauss, J. Schröder, and B. J. Eggleton, “Non-degenerate two-photon absorption in silicon waveguides: analytical and experimental study,” *Optics Express* **23**, 17,101–17,110 (2015).
5. S. Grillanda and F. Morichetti, “Light-induced metal-like surface of silicon photonic waveguides,” *Nature Communications* **6** (2015).
6. I. Aldaya, A. Gil-Molina, J. L. Pita, L. H. Gabrielli, H. L. Fragnito, and P. Dainese, “Nonlinear carrier dynamics in silicon nano-waveguides,” *Optica* **4**, 1219–1227 (2017).
7. R. Soref and B. Bennett, “Electrooptical effects in silicon,” *IEEE Journal of Quantum Electronics* **23**, 123–129 (1987).
8. C. Monat, B. Corcoran, D. Pudo, M. Ebnali-Heidari, C. Grillet, M. D. Pelusi, D. J. Moss, B. J. Eggleton, T. P. White, and L. O’Faolain, “Slow light enhanced nonlinear optics in silicon photonic crystal waveguides,” *IEEE Journal of Selected Topics in Quantum Electronics* **16**, 344–356 (2010).
9. A. D. Bristow, N. Rotenberg, and H. M. Van Driel, “Two-photon absorption and Kerr coefficients of silicon for 850–2200 nm,” *Applied Physics Letters* **90**, 191,104 (2007).